ELSEVIER

Tectonophysics 277 (1997) 285–306

TECTONOPHYSICS

Geometry and style of partitioned deformation within a late Cenozoic transpressional zone in the eastern Gobi Altai Mountains, Mongolia

W. Dickson Cunningham [a,*], Brian F. Windley [a], Lewis A. Owen [b], Tiffany Barry [a], D. Dorjnamjaa [c], J. Badamgarav [c]

[a] *Department of Geology, University of Leicester, Leicester, LE1 7RH, UK*
[b] *Department of Geography, Royal Holloway, University of London, London, UK*
[c] *Mongolian Academy of Sciences, Institute of Geology, Ulaan Bator, Mongolia*

Received 7 August 1996; accepted 10 February 1997

Abstract

The Gobi Altai is the easternmost extension of the Mongolian Altai and consists of topographically discontinuous E–W-trending ranges with peaks averaging 2000–3000 m in elevation. The region is seismically active and characterized by prominent E–W left-lateral strike-slip faults that localize transpressional deformation and uplift along their lengths and at stepover zones. This report summarizes structural field investigations made in the easternmost Gobi Altai to document the structural geometry and style of late Cenozoic transpressional deformation in the region in order to better understand processes of intracontinental mountain building and the distant intracontinental strain response to the Indo–Eurasian collision.

The Artsa Bogd range marks the northeastern terminus of the Gobi Altai and is topographically asymmetric with a high northern margin marked by N-vergent thrust faults and left-lateral oblique-slip faults. The northern side of the range is also bounded by a foreland basin that contains N-vergent thrust faults and folds that deform Quaternary sediments. The southern margin of Artsa Bogd appears tectonically inactive but contains S-vergent thrust faults and left-lateral wrench zones. The range appears to have a flower structure cross-sectional geometry that may reflect transpressional inversion of a Mesozoic basin. The isolated, high and narrow Tsost Uul range south of Artsa Bogd occupies a restraining bend position along the left-lateral Tsost Uul strike-slip fault system. Major faults within the range define a half-flower structure cross-sectional geometry. To the south of the Tsost Uul range, the Gobi Bulag left-lateral strike-slip fault system is marked by small push-up ridges and one major restraining bend mountain where the fault steps to the right near its western end. Throughout the region, Late Cretaceous–Tertiary basalts and Tertiary and Quaternary sediments are deformed by the major fault systems indicating late Cenozoic fault activity.

These fault systems and the ranges formed along them occur at fairly regular intervals (approximately 20 km) between the North Gobi Altai fault system and the Gobi Tien Shan fault system, two major left-lateral strike-slip faults that cut across southern Mongolia. Together the faults define a parallel array of discrete linear belts of Cenozoic E–W left-lateral transpressional deformation south of the Hangay Dome. The regular spacing of the fault systems may suggest more uniform distributed left-lateral flow at depth. Eastward-directed lower crustal and lithospheric mantle flow is suggested by

* Corresponding author. Tel.: +44 (116) 252-3649; Fax: +44 (116) 252-3918; E-mail: wdc2@le.ac.uk

PII S0040-1951(97)00034-6

existing seismic anisotropy data for the eastern Gobi Altai and is believed to be the driving force for the upper crustal deformation.

Keywords: Mongolia; Altai; transpression; mountain building; orogenesis

1. Introduction

The Artsa Bogd region of the eastern Gobi Altai Mountains of southern Mongolia (Fig. 1) lies between two major (>350 km length) E–W left-lateral strike-slip fault systems, the North Gobi Altai fault system and the Gobi Tien Shan fault system (Figs. 2 and 3). These active fault systems are believed to be accommodating a small fraction of the intracontinental strain caused by the distant Indo–Eurasian collision 2500 km to the south (Tapponnier and Molnar, 1979; Cunningham et al., 1996a; Fig. 3). Previous field investigations, analysis of satellite imagery and review of existing literature for the Gobi Altai indicate that the region defines a corridor of left-lateral transpressional tectonic activity during the late Cenozoic (Cunningham et al., 1996a). Field work was carried out in the Artsa Bogd region to better understand general processes of intracontinental, intraplate mountain building and the fault geometries that have constructed the eastern Gobi Altai. This report connects with previous studies in Mongolia including Cunningham and Windley (1995), Cunningham et al. (1996a,b), and Owen et al. (1997).

1.1. Regional geologic setting

The Gobi Altai is the southeastern extension of the Altai range and consists of topographically discontinuous E–W-trending ranges generally reaching 2000–3000 m elevations with a few ranges exceeding 3500 m. The mountain ranges terminate to the east and southeast. The region has a basin and range physiographic appearance and is increasingly arid towards the south. Outcrop exposure is generally excellent. Many of the ranges have sharply defined mountain fronts indicating active faulting and uplift. Active strike-slip, oblique-slip and thrust faults have been identified whereas active normal faults have not been documented in the Gobi Altai. The overall late Cenozoic deformation regime appears to be transpressional and the highest ranges in the region are

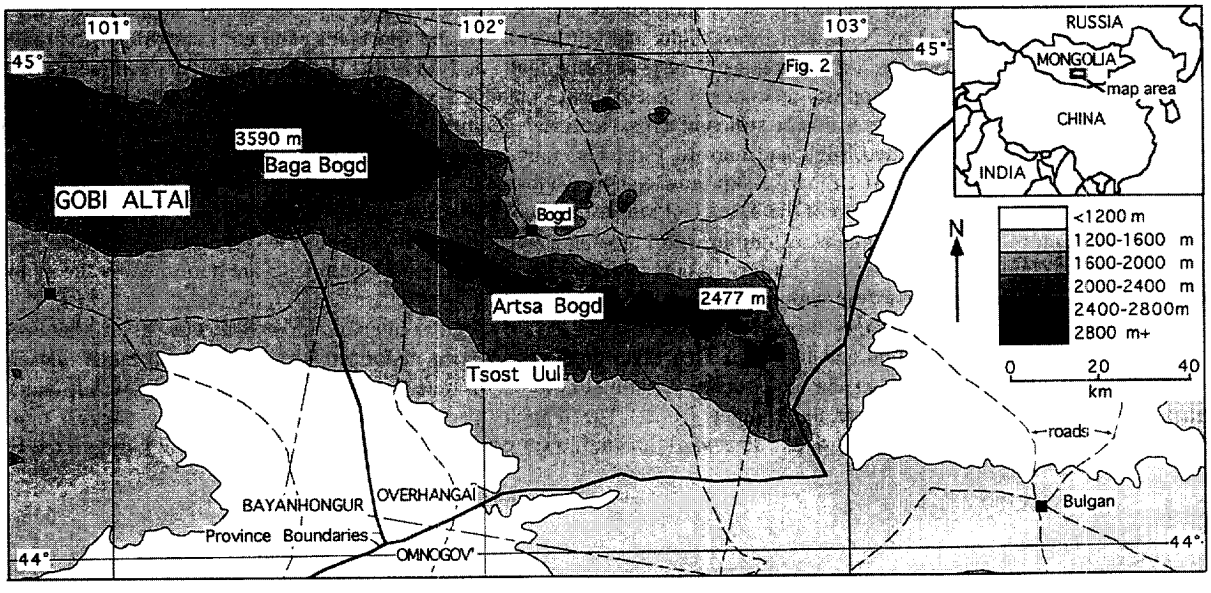

Fig. 1. Topographic map of the Artsa Bogd region of the eastern Gobi Altai, Mongolia.

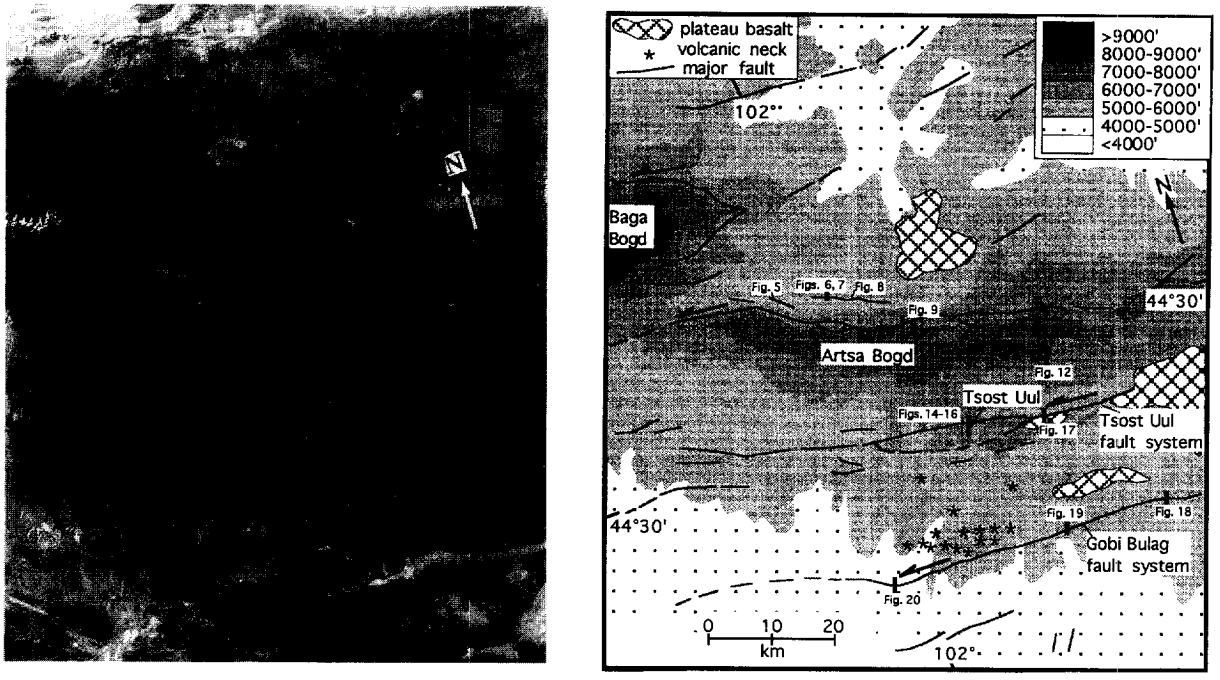

Fig. 2. Landsat image and geological interpretation of major faults visible on image in the Artsa Bogd region of eastern Gobi Altai. Location of subsequent figures shown. Location of satellite image shown in Fig. 1.

restraining bend uplifts along the seismically active North Gobi Altai fault system (Cunningham et al., 1996a).

The basement rocks of the eastern Gobi Altai consist of discontinuous exposures of Palaeozoic low-grade metasedimentary rocks, volcaniclastic sedimentary rocks, carbonates and isolated felsic intrusions that are thought to represent arc basement, arc-derived sediment and continental platform material (Fig. 4; Zorin et al., 1993; Sengör et al., 1993; Lamb and Badarch, 1995). Northwards structural vergence of Palaeozoic folds and thrust nappes in southern central Mongolia suggests late Palaeozoic northwards collision and overthrusting of an arc terrane and microcontinent (South Gobi microcontinent) against the Baidrag massif (Dergunov, 1989) that forms the basement to central Mongolia (Suyetenko et al., 1978; Tikhonov and Yarmolyuk, 1982; Ruzhentsev and Badarch, 1989; Zorin et al., 1993). Superimposed on the Palaeozoic contractional history is a period of early Mesozoic clastic sedimentation in a foreland basin probably related to Jurassic contraction in northern China and extreme southern Mongolia (Hendrix et al., 1996). Late Jurassic and Cretaceous continent-derived clastic and local volcanic rocks that were deposited during a period of intraplate extension and volcanism lie unconformably on deformed Palaeozoic and early Mesozoic rocks (Shuvalov, 1969; Samoylov et al., 1988; Traynor and Sladen, 1995). Peneplanation of the region is believed to have occurred in the latest Cretaceous and early Tertiary (Devyatkin, 1974, 1975).

The onset of Cenozoic deformation in the Gobi Altai is not well constrained but based on sedimentological grounds is thought to have begun in the mid-late Tertiary (Baljinnyam et al., 1993), possibly at the end of the Oligocene (30–25 Ma; Devyatkin, 1974, 1975). This deformation is characterized by development of through-going E–W left-lateral strike-slip faults, NW–SE-directed contraction and block uplift. Much of what is known about the Cenozoic tectonic activity derives from the important and prescient Landsat-based analysis by Tapponnier and Molnar (1979) and studies of major earthquakes, active fault scarps and Cenozoic sedimentary deposits in Mongolia by Devyatkin (1974, 1975), Khilkho et al. (1985) and Baljinnyam et al. (1993). Historical seismicity is unknown from the Artsa Bogd region;

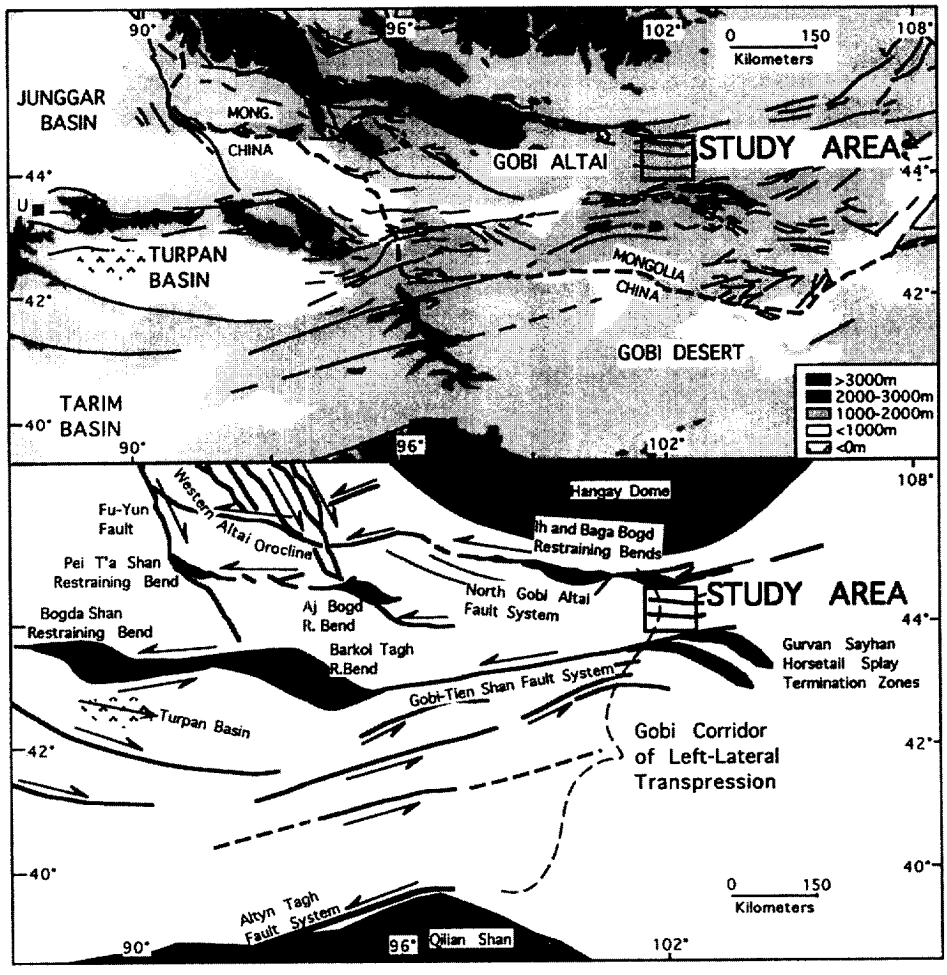

Fig. 3. Regional fault systems in southern Mongolia and adjacent areas of China (adapted from Cunningham et al., 1996a). Region investigated in this study occurs within a wider E–W corridor of late Cenozoic left-lateral transpressional deformation and localized uplift between the Hangay Dome and Qilian Shan.

however, the great 1957 $M = 8.3$ left-lateral earthquake occurred less than 100 km to the northwest in the Ih Bogd/Baga Bogd ranges (Florensov and Solonenko, 1963; Bayarsayhan et al., 1996) along the North Gobi Altai fault system (Fig. 2). Cunningham et al. (1996a) presented preliminary structural studies of transpressional deformation along the North Gobi Altai and Gobi Tien Shan fault systems and documented the important role the strike-slip faults have played in localizing late Cenozoic uplift. Investigations into the tectonic geomorphology of the Artsa Bogd region by Owen et al. (1997) indicate active but low (0.1–1 m/ka) late Quaternary uplift rates along the Artsa Bogd and Tsost Uul mountain fronts. Limited late Cenozoic volcanism has also occurred in the region possibly indicating local zones of transtension/extension (Yarmolyuk et al., 1991). The extent to which Cenozoic uplift has occurred along reactivated older structures is a major unresolved problem in the Gobi Altai region.

Three main regions were examined within the study area and will be discussed below: the Artsa Bogd range, the Tsost Uul range and the Gobi Bulag fault zone.

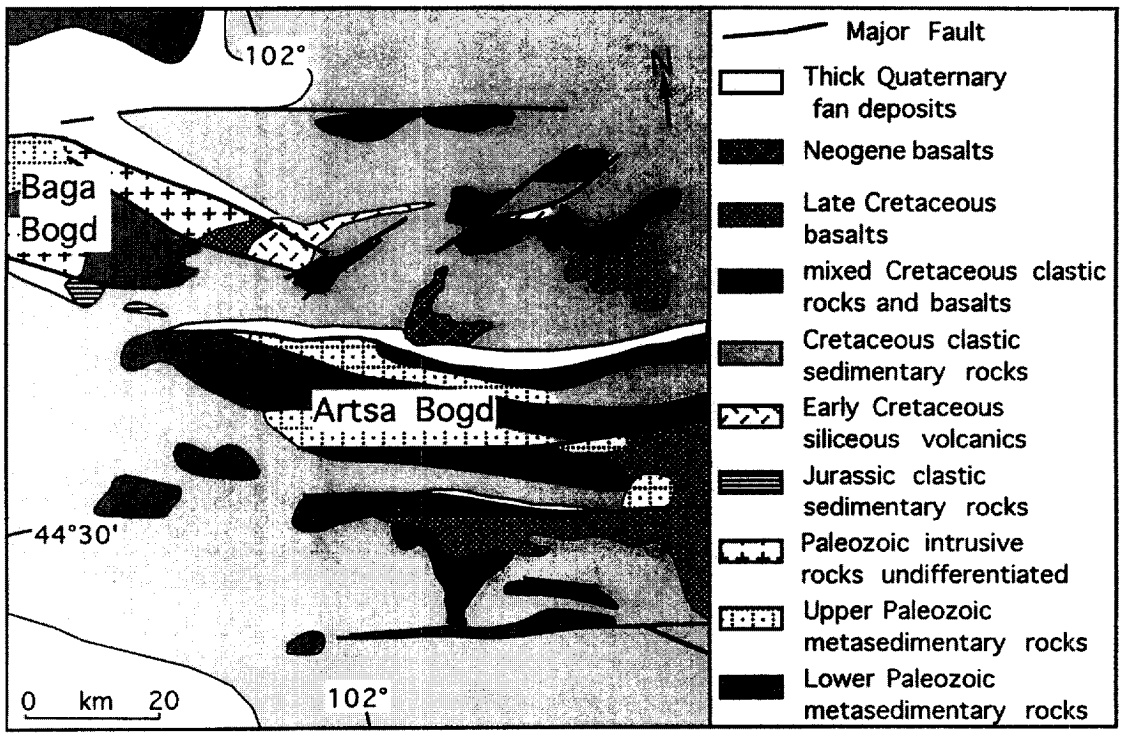

Fig. 4. Simplified geologic map of the Artsa Bogd region, eastern Gobi Altai. Map adapted from Samoylov et al. (1988).

2. Artsa Bogd

Artsa Bogd sits at the northeastern end of the Gobi Altai as an isolated block with a broad bajada on its northern and southern sides. The northern side of the range is sharply defined on Landsat imagery for most of its length as a topographic escarpment with a low mountain front sinuosity (Bull and McFadden, 1977), suggesting recent fault activity (Fig. 2). The front is mantled by coalescing debris cones of Holocene age. Many of these cones are actively aggrading by debris flow processes. Areas along the front where debris cones are absent are locally marked by springs. The southern side of the range has a high mountain front sinuosity and lacks fresh fault scarps suggesting that it is tectonically inactive (Fig. 2). The topography of the range is strongly asymmetric with highest elevations and steepest relief near the northern front and gentle S-sloping topography on the southern side. Furthermore, valleys incised into the northern side of Artsa Bogd have a much smaller valley-floor width to valley-height ratio than those on the southern side. This supports the view that the northern side is more active than the southern side of Artsa Bogd. Several small N–S structural transects were made along the northern side of Artsa Bogd and across small ridges within the broad alluvial valley north of the range to better understand the range's frontal structure. One small transect was also completed across the range's southern margin (Fig. 2).

A small upright anticline (wavelength approximately 300–400 m) that folds fanglomerates and red sandstones occurs directly north of the frontal escarpment near the western end of Artsa Bogd (Fig. 5). The fold plunges shallowly southeast (07°/140), oblique to the trend of the mountain front. Another SE-plunging anticline (09°/114, wavelength >750 m) that trends oblique to the mountain front is present en echelon to the previous fold approximately 7 km further west. This fold exposes red sandstones in the core that are overlain by fanglomerates and sandstones. The fold is highly asymmetric with a steep northern limb and shallow southern

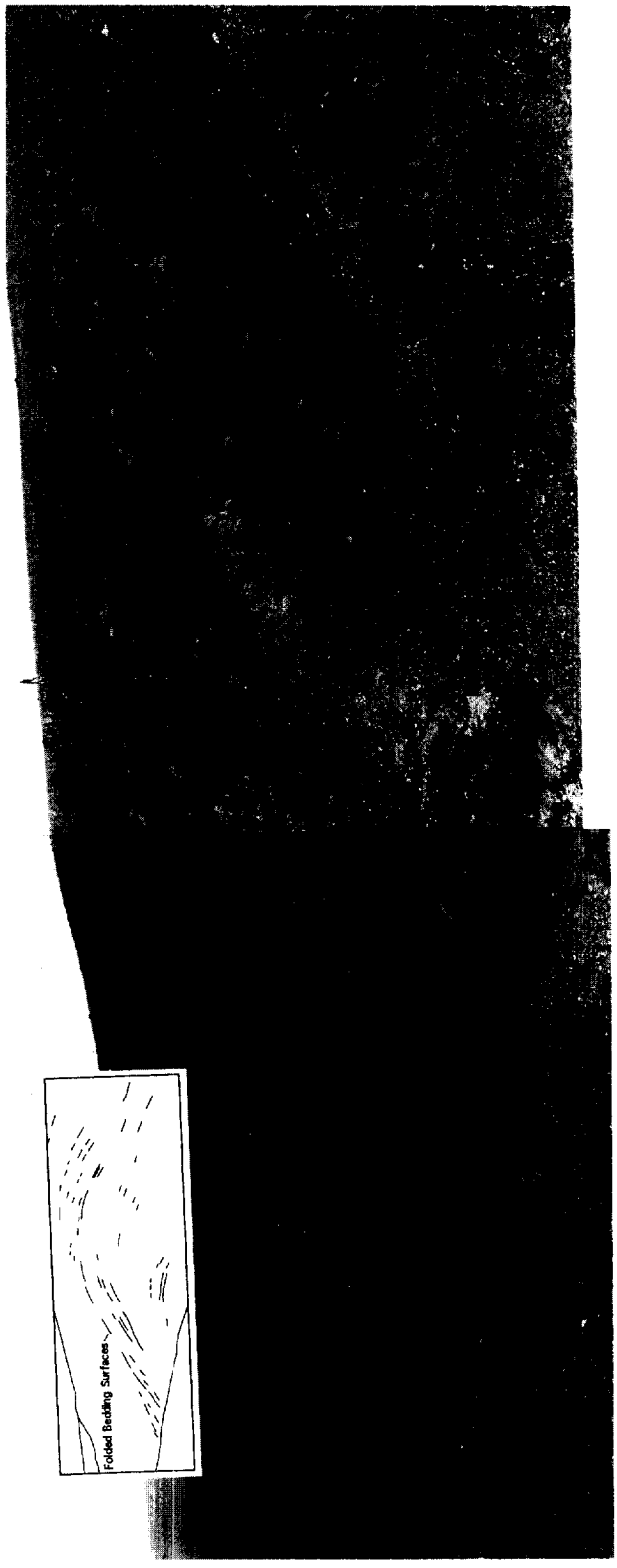

Fig. 5. Photo looking east of frontal anticline in the Artsa Bogd foreland, northern side of range. Inset highlights visible folded bedding surfaces. Width of photo approximately 100 m. Note person on skyline for scale. Location of photo shown in Fig. 2.

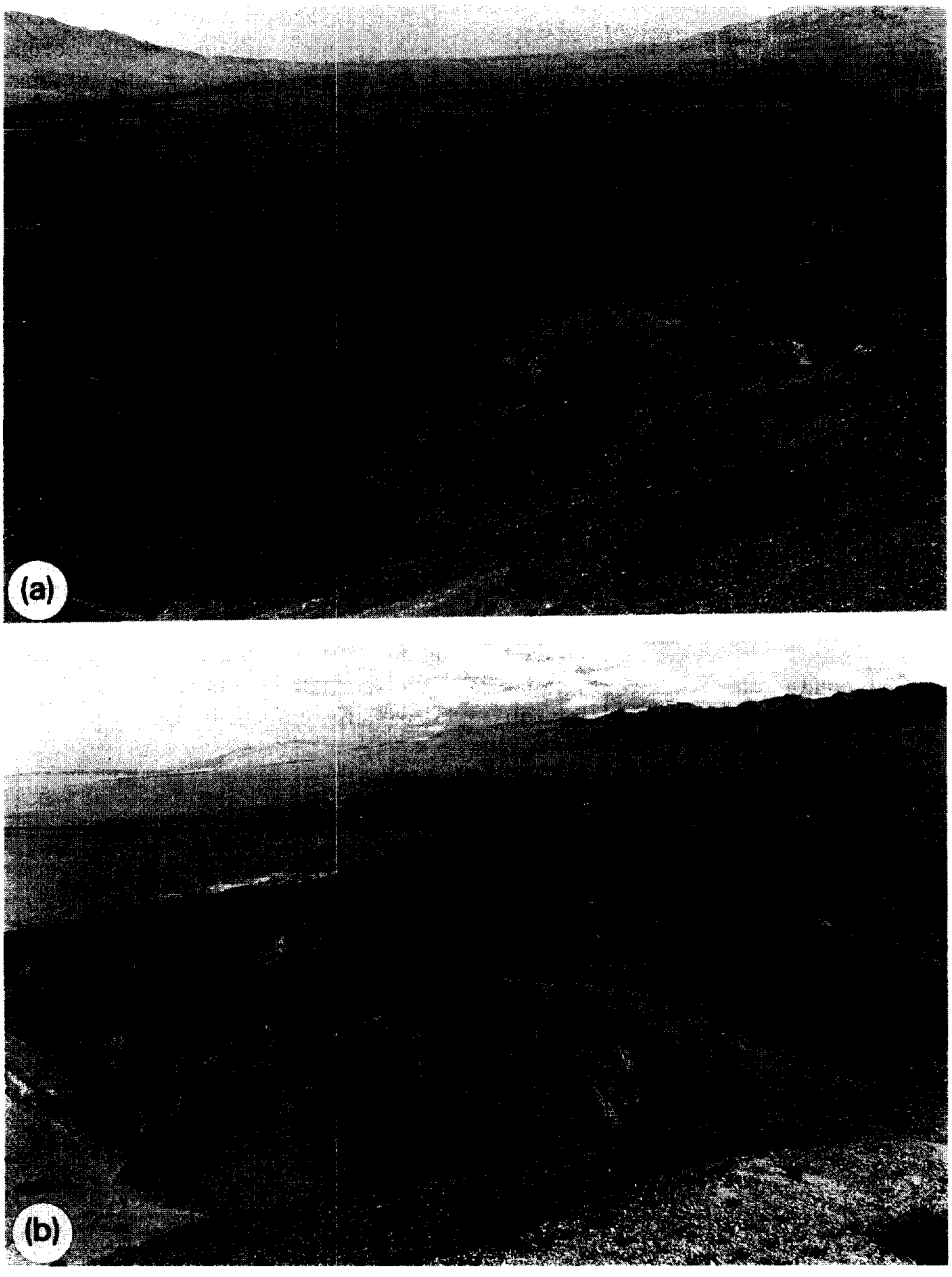

Fig. 6. (a) Photo looking west of narrow ridge north of Artsa Bogd. Ridge is composed of tilted and thrusted clastic sedimentary rocks (brown and white tones) and micritic limestone (black). Thrusts strike E–W and dip steeply north. Area of Fig. 7 map and cross section follows drainage 1/3 up from bottom of photo. Western end of northern mountain front of Artsa Bogd visible in distance on left. Southeastern end of Baga Bogd range visible in top right corner. Location of photo shown in Fig. 2. (b) Photo looking east of same ridge as in (a). Photo shows steeply S-dipping clastic strata and water gap in ridge in distance where fault shown in Fig. 8 is exposed (approximately 4 km away from where photo was taken). Location of photo shown in Fig. 2. Northern mountain front of Artsa Bogd visible in distance.

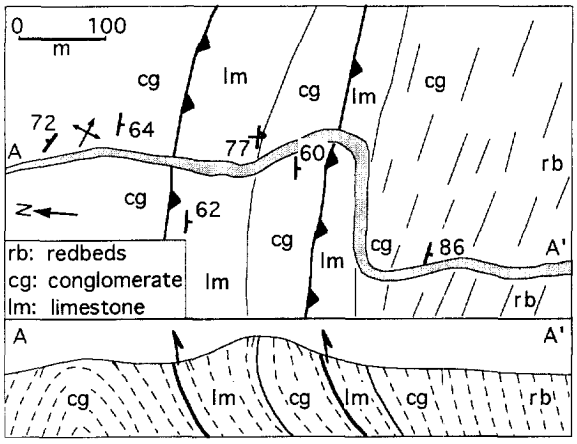

Fig. 7. Small geologic transect map and cross section across narrow ridge that lies in the Artsa Bogd foreland, northern side. Location of map shown in Figs. 2 and 6a.

limb. Unconsolidated Quaternary alluvial deposits are gently arched on the crest of the fold suggesting that deformation continued until recently and may be still active. The folded sandstones are not dated but are petrologically and sedimentologically similar to Mesozoic red clastic rocks that are common in the region (Shuvalov, 1969) or are possibly Tertiary sediments shed off of Artsa Bogd and later deformed.

A separate sub-linear ridge occurs several km north of Artsa Bogd's frontal escarpment near the lowest point of the alluvial valley along the range's northern side (Figs. 2 and 6). This ridge is composed of alternating red and tan sandstones, pebble conglomerates and black micritic limestones. Fig. 7 is a short transect across the western end of the ridge showing the structural repetition of the black micritic limestone along two steeply S-dipping thrust faults (Fig. 7). Folded conglomerate beds north of the thrust zone may indicate a third blind thrust at depth.

Four kilometres to the east, the along-strike continuation of the thrust system is exposed where the ridge is dissected by a small stream (Fig. 8). In the stream cut (44°38′27.8″N, 102°07′18.8″E; Fig. 8) a series of curving sub-vertical, north-vergent reverse faults displace a sequence of poorly indurated silts, sands and red pebble beds that onlap the main red marlstone that comprises the ridge. Slickensides are almost pure down dip on all fault surfaces indicating that faulting was of pure thrust-type without a strike-slip component. The measured displacements

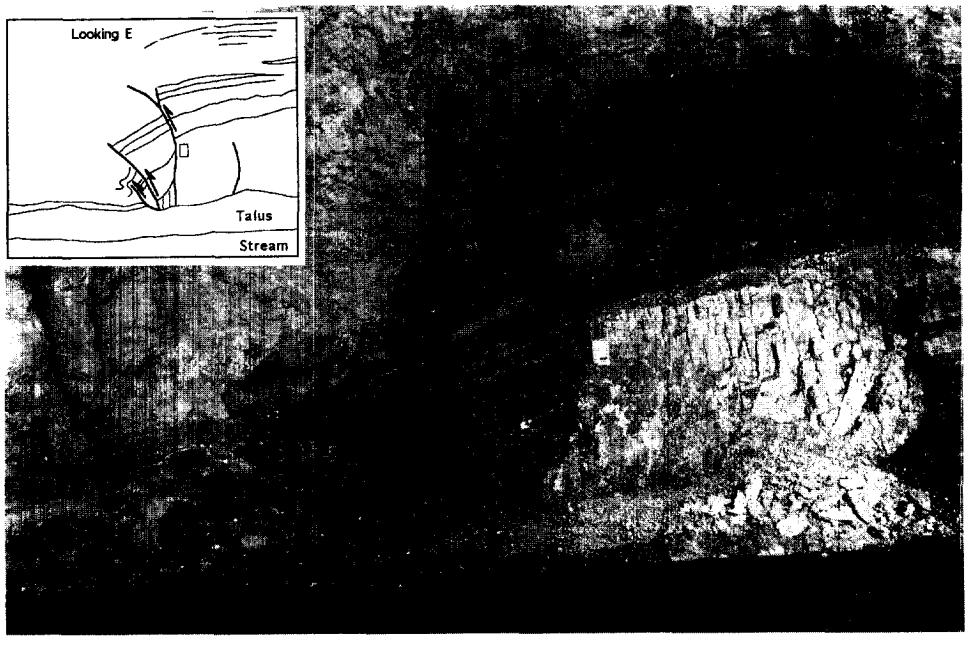

Fig. 8. View looking east of vertical fault zone showing southern-side up thrust motion. Fault is exposed along stream that cuts through narrow ridge that lies in the Artsa Bogd foreland, northern side. Fault cuts Tertiary clastic rocks and Quaternary alluvial deposits. Location of photo shown in Figs. 2 and 6b.

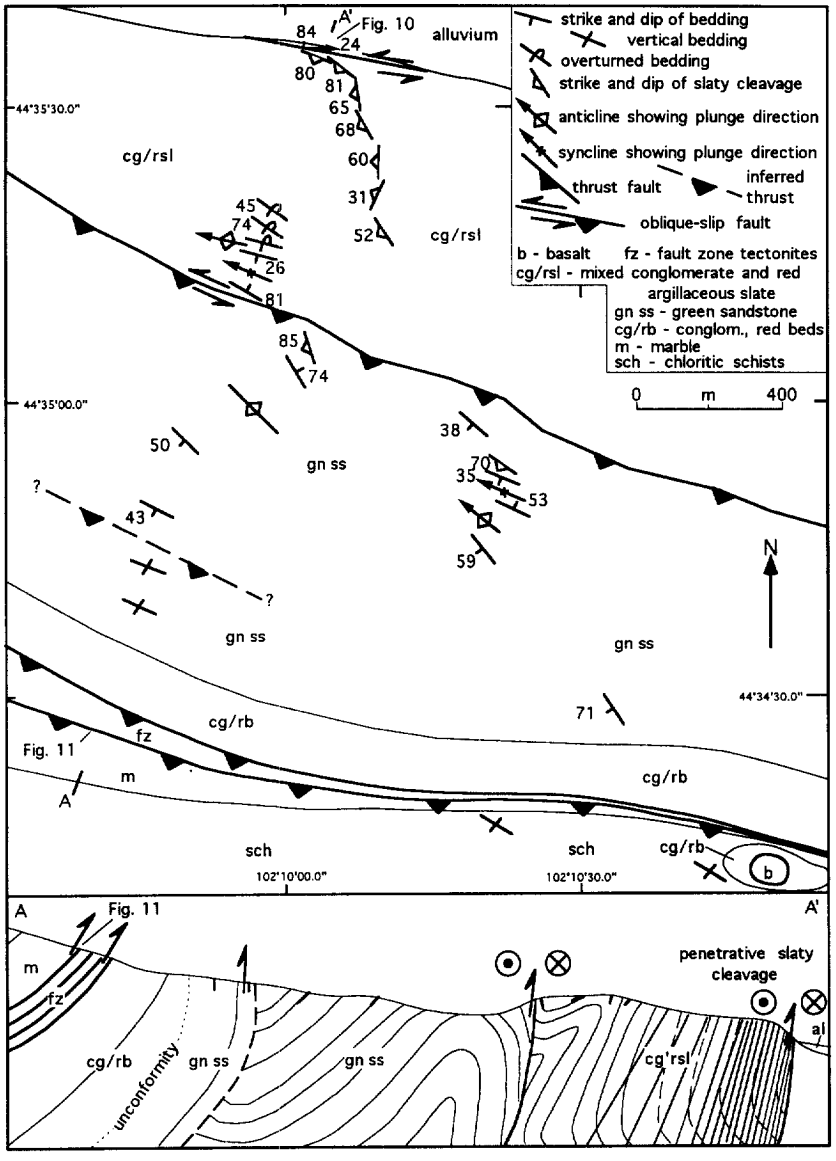

Fig. 9. Geologic map and cross section of northern Artsa Bogd at approximately 44°35′N, 102°10′E. Location of map shown in Fig. 2.

are approximately 2 m but the total displacement is probably significantly more because the sediments that are cut were deposited during Quaternary time (Owen et al., 1997) after the fault initiated movement. Furthermore, the upper plate to the fault has been thrust up to form a ridge that is locally 100 m higher than the surrounding plain. The deformed sedimentary rocks are undated but differ from the more massive and better indurated Mesozoic clastic sequence found throughout the region (Shuvalov, 1969). Thus they are interpreted to be Neogene or Quaternary alluvial and fluvial deposits locally derived from Artsa Bogd (Owen et al., 1997). The faults displace sediments within 50 cm of the surface and fold the topmost beds suggesting that they may still be active.

Fig. 9 shows a geological map and cross section of a transect through the northern side of the main

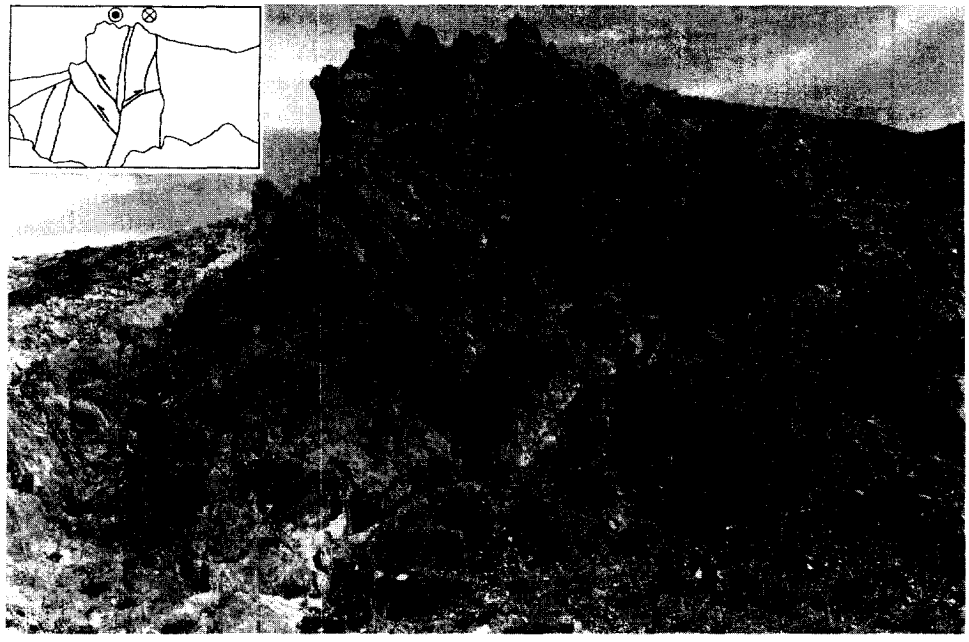

Fig. 10. Flower-like fault geometries along northern Artsa Bogd mountain front. Small rucksack in foreground gives scale. Location of photo shown in Fig. 9. Inset highlights fault splay geometry. Main vertical fault strikes 280, dips 74° NE and has slickensides plunging 24°/093.

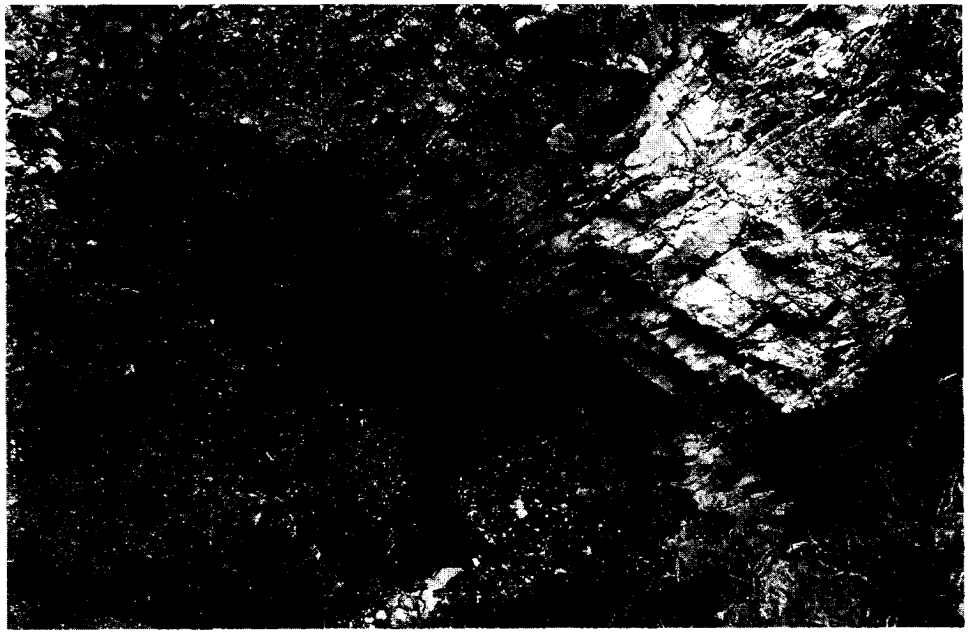

Fig. 11. View southeast of brittle N-vergent thrust fault emplacing massive white marble above highly sheared bluish-grey chloritic phyllite. Field notebook under overhang for scale. Fault zone is over 100 m wide. Location of photo shown in Fig. 9.

Artsa Bogd range. At the northernmost end of the transect (44°35′N, 102°10′E), the mountain front is marked by a steep brittle fault zone with both north- and south-branching thrust faults rooted into the zone (Fig. 10). The steep master fault strikes 280°, dips sub-vertically and has slickensides plunging 24°/093 indicating dominantly strike-slip displacement. The entire zone has a flower structure geometry suggesting that the frontal fault system for Artsa Bogd at this location is transpressional. Apparent deflection of slatey cleavage into near parallelism with this zone (Fig. 9) suggests left-lateral displacement along the fault; however the change in cleavage trend could also be related to older unrelated deformation.

A second steep fault zone that is approximately 1 km south of the northern mountain front places undated green volcaniclastic sandstones over a sequence of alternating green conglomerates and red argillaceous slates. This zone has an important and possibly dominant strike-slip component along it as indicated by stretched pebbles from within the fault zone that are elongate parallel to strike (NW) and contain asymmetric tails of chloritic overgrowth indicating left-lateral motion. Measured pebble dimension $X:Y:Z$ ratios from within the zone are typically 3:2:1 to 4:2:1 indicating flattening strains within the fault plane and extension along strike. Immediately north of the fault zone several N-vergent folds occur that contain an axial planar cleavage that increases in intensity of development towards the northern mountain front.

A third major fault occurs several kilometres into the range (Figs. 9 and 11). It dips moderately south-southwest and has a strongly tectonized zone over 100 m thick. It places massive white Silurian–Devonian marbles that are overlain by chloritic schists above highly sheared bluish-grey chloritic phyllites that grade downwards into brecciated coarse conglomerates. Asymmetric N-vergent folds within the fault zone as well as the juxtaposition of higher-grade chloritic schists in the upper plate indicate N-vergent thrusting shear sense.

These structures suggest that the northern front of Artsa Bogd in this location has been constructed by N-vergent thrust faults in the interior and steep left-lateral oblique-slip faults along the northern margin. The overall geometry suggests transpressional uplift with the strike-slip component partitioned along the northern 1 km of the range. Differentiating the older Palaeozoic deformational history from Mesozoic(?) or Cenozoic deformation is difficult because all major structures including folds in the basement lithologies are N-vergent. In the southeastern corner of the map area (Fig. 9), an isolated mountain is capped by red sandstones and a vesicular basalt flow that lie unconformably above the chlorite schists. These units are gently buckled on the upper plate to the thrust zone suggesting that thrusting postdated their deposition. Late Cretaceous–Tertiary basalt flows are common in the region (Figs. 2 and 4) and Berkey and Morris (1927) and Samoylov et al. (1988) report an extensive S-dipping sequence of Late Cretaceous–Tertiary basalt flows on the S-facing slope of eastern Artsa Bogd that have been tilted since their eruption. If the basalt flow remnant shown in Fig. 9 is a part of the more widespread series of flows exposed to the south and east, then the thrust faults structurally below the basalts must be post-Late Cretaceous.

Fig. 12 shows a small transect across the southern topographic boundary to the range (Fig. 12). The dominant lithologies are strongly cleaved Permian green chloritic slates and phyllites. They are cut by numerous brittle faults that record dominantly S-vergent thrust and left-lateral oblique-slip displacement.

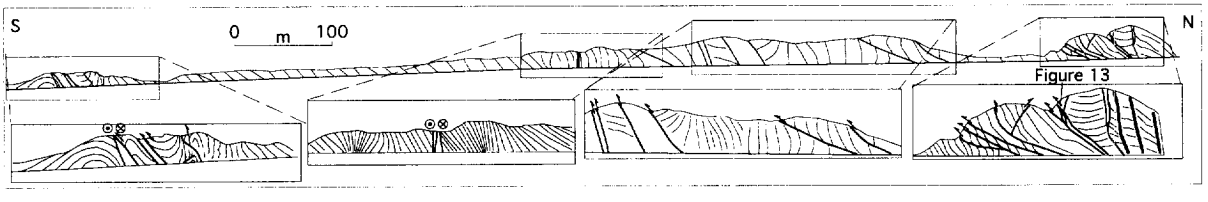

Fig. 12. Cross section of transect along southern side of Artsa Bogd at 44°28′04.5″N, 102°20′56.2″E, showing major faults and orientations of bedding. S-vergent thrust and oblique-slip faults suggest transpressional wrench fault systems define the southern boundary to the range. Location of transect shown in Fig. 2.

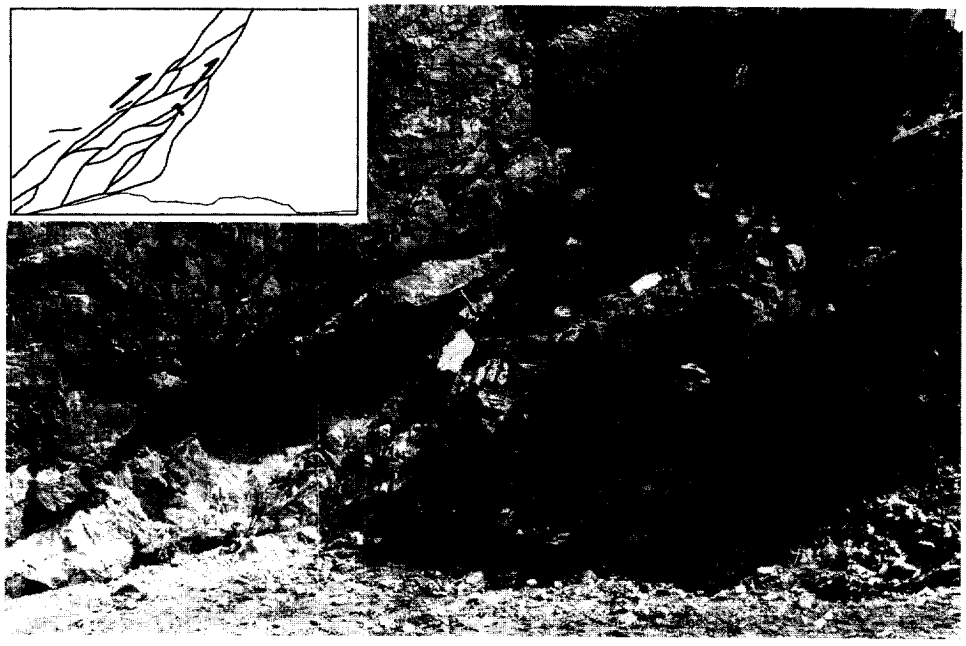

Fig. 13. Photo looking east of S-vergent brittle thrust fault from the S Artsa Bogd structural transect (Fig. 12). Location of photo shown in Fig. 12. Thrusts cut Palaeozoic slates and weakly metamorphosed volcaniclastic sedimentary rocks.

At the southernmost margin, folded phyllites are cut by two separate left-lateral wrench zones that are separated by a zone of homoclinally dipping phyllite. Farther north, shallow- to moderate-dipping S-vergent thrusts are numerous (Figs. 12 and 13) and cut through all units including an important feldspar porphyritic mafic dyke swarm that strikes between 000 and 070 and dips steeply. The dykes increase in volume towards the centre of the range until they constitute approximately 75% of the country rock. Although they have not been dated, they may represent feeder conduits for some of the extensive Cretaceous–Tertiary plateau basalts that occur along the southern slopes of Artsa Bogd and to the north and south of the range (Figs. 2 and 4). If this interpretation is correct, then the thrust faults that cut the dykes are post-Late Cretaceous in age.

In summary, the major faults that were identified within the valley north of Artsa Bogd and along the northern front of Artsa Bogd indicate N-directed shortening with a local left-lateral strike-slip component. All the faults are moderate- to high-angled and none are shallow (30° or less) dipping structures. The presence of small alluvial cones along the northern Artsa Bogd front, the sharply defined front as seen on Landsat imagery, and folding and faulting of Tertiary and Quaternary sedimentary deposits and Late Cretaceous–Cenozoic basalts indicates that this deformation is post-Mesozoic and probably Neogene to Recent.

3. Tsost Uul

The Tsost Uul range, south of Artsa Bogd, is a topographic culmination along the E–W-trending Tsost Uul fault system. The highest elevations in the range are rugged mountains composed of Silurian marble and siliceous limestone that show up as light tones on the Landsat image (Fig. 2). These highest mountains occur in a gentle right-stepping bend along the trend of the fault system. The fault system itself can be traced for over 70 km on the Landsat image (Fig. 2).

Figs. 14 and 15 show a transect across the range. The southern boundary to the range is an impressive vertical fault zone that separates white marbles to the south from brown calc-silicates, calcareous sandstones and limestones to the north. The fault plane is spectacularly exposed and strikes 084 and dips 85°SE with slickensides plunging 14°/085 (Figs. 14–

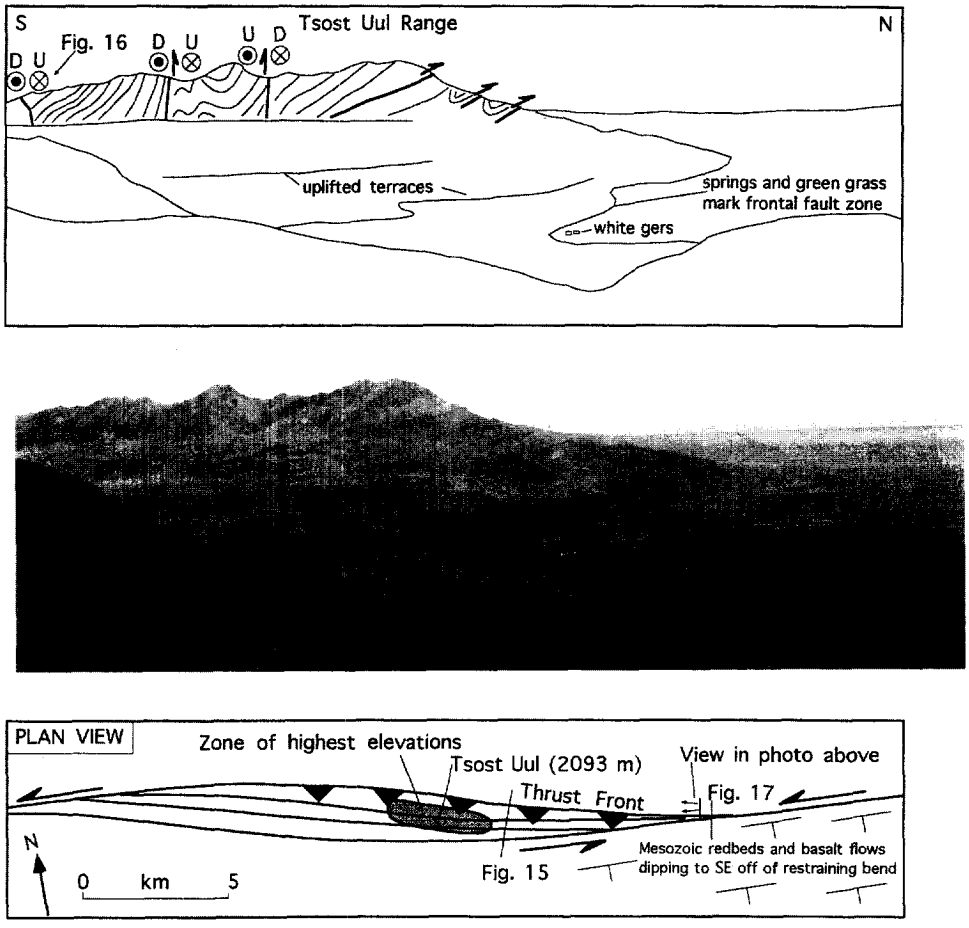

Fig. 14. Distant view looking west of Tsost Uul range showing prominent structural features and frontal fault system delineated by springs and green grass (dark tones). Width of photo along summit ridge line is approximately 8 km. Fault geometries suggest that the range has an asymmetric flower structure cross-sectional geometry and has formed along a transpressional bend in the Tsost Uul left-lateral strike-slip fault system. See Fig. 2 for location of photo and Landsat view.

16). The fault zone is bounded by up to 10 m of brecciated wall rock and locally is N-dipping at an angle of 80–90°. The steepness of the fault plane and shallow plunge of the slickensides (Fig. 16) indicate that the fault is of strike-slip type with a small dip-slip component of motion. The fault is interpreted to be left-lateral because the slickensided surfaces step downwards to the west when viewing the vertical fault surface from the north (Fig. 16c). In addition, the fault is subparallel to other left-lateral fault systems identified in the region (Baljinnyam et al., 1993; Cunningham et al., 1996a) and the along-strike relationship between topography and fault orientation along the Tsost Uul fault system indicates that uplift has occurred where the fault is right-stepping (Figs. 2 and 14).

North of the southern bounding strike-slip fault, the interior of the range is cut by two other E-striking, steeply dipping faults. Oblique-slip slickensides and dragged bedding adjacent to the fault zones indicate components of reverse motion. The faults bound blocks comprised of carbonate and sandstone units that are deformed into open to tight (0.05–0.5 km wavelength), upright folds that generally plunge shallowly eastwards. The northern front of the range is marked by a thick, massive, white marble unit that is thrust northwards over tightly folded green sandstones and brown calcareous sandstones. Smaller

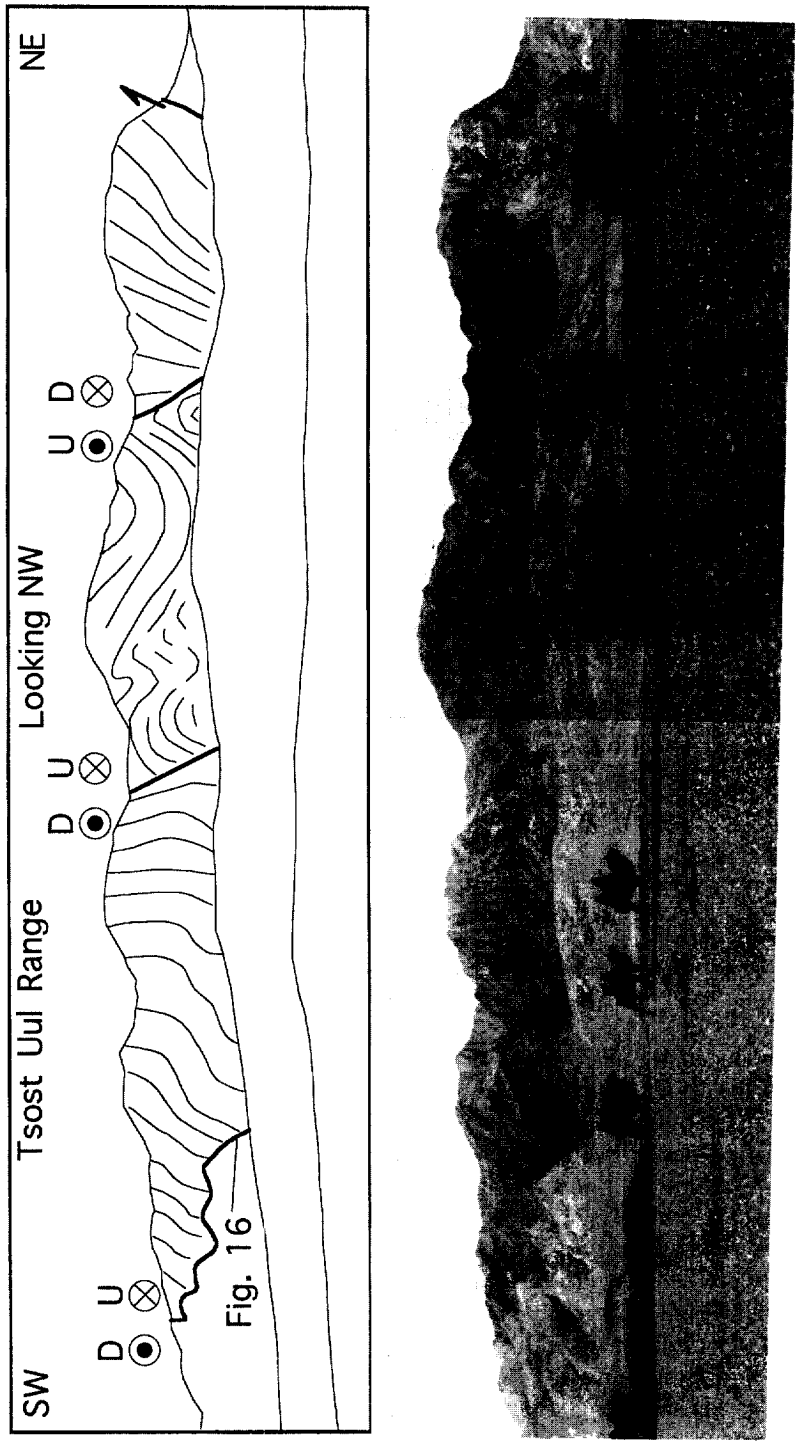

Fig. 15. Close-up view looking northwest of the Tsost Uul range showing major structural features and structural interpretation based on field checks made within range. Location of photo shown in Fig. 2. Width of photo approximately 5 km.

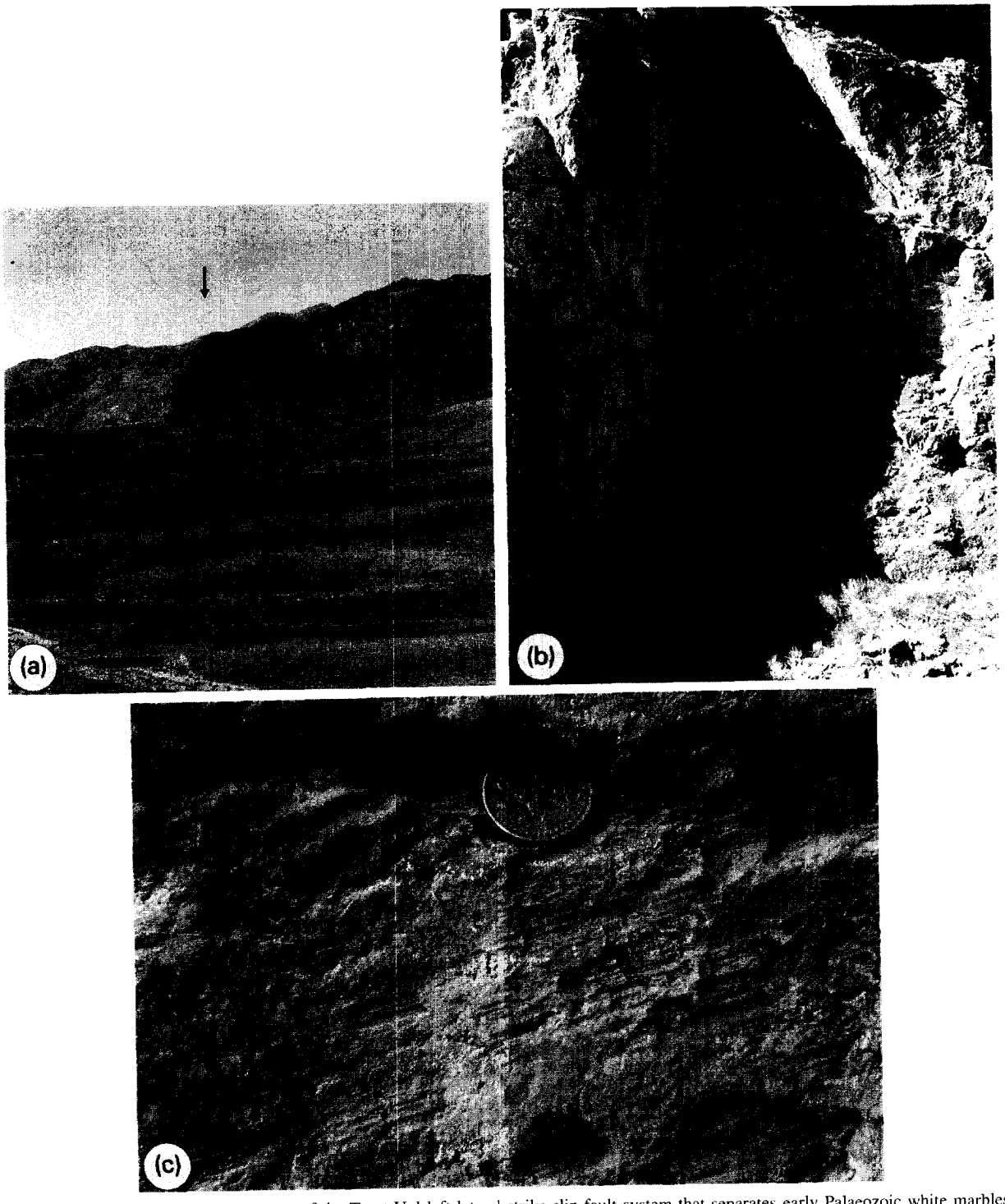

Fig. 16. (a) Distant view looking west of the Tsost Uul left-lateral strike-slip fault system that separates early Palaeozoic white marbles (southern side) from brown calc-silicates, calcareous sandstones and limestones (northern side). Location of photo shown in Fig. 15. (b) View looking west of spectacularly exposed Tsost Uul left-lateral strike-slip fault vertical fault plane. Width of photo approximately 15 m. (c) Close-up of Tsost Uul left-lateral strike-slip fault plane showing shallowly E-plunging slickensides on fault surface indicating dominantly strike-slip motion.

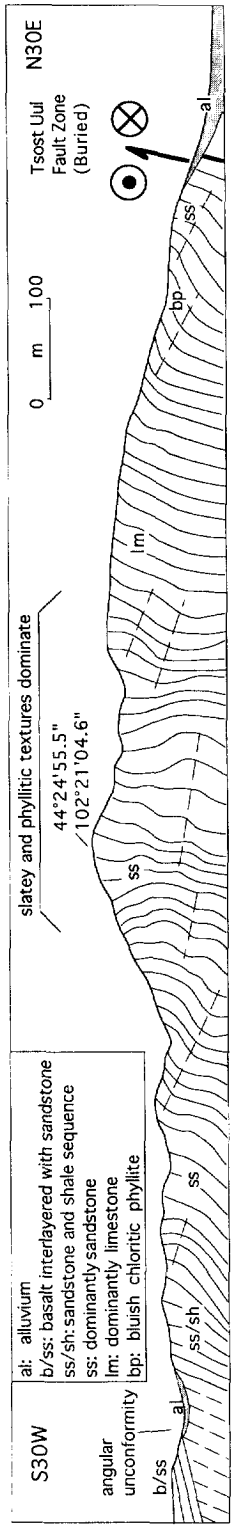

Fig. 17. Transect across small ridge along the Tsost Uul fault system. Location of figure shown in Figs. 2 and 14.

N-vergent thrust faults occur within the folded sandstones. The most northerly of these faults delineates the front of the range and locally is marked by springs (Fig. 14).

Fig. 17 shows a transect across a small mountain that forms the easternmost ridge of the Tsost Uul uplifted area. The southern side of the ridge is overlain by a series of shallowly SE-dipping Cretaceous basalt flows and intercalated red beds (Samoylov et al., 1988). These basalt flows unconformably overlie a Palaeozoic sequence of more steeply dipping green and brown sandstones, chloritic slates and phyllites, and siliceous marbles that form the ridge. The sequence is consistently SE-dipping despite gentle undulations and minor folds that generally verge south (Fig. 17). Sheared bluish chloritic phyllite and local zones of brecciated sandstone along the northern mountain front suggest that it marks a buried fault zone. No scarp is present, however, and no evidence was seen for recent faulting.

These preliminary observations suggest that the Tsost Uul range has formed by transpressional uplift along oblique-slip and thrust faults at a gentle restraining bend along the Tsost Uul fault system (Fig. 14) The southeasterly dipping Cretaceous basalts tilt off of this zone of uplift indicating that uplift is post-Cretaceous. The southeastern plunges of most folds in the interior of the Tsost Uul range are also consistent with the restraining bend interpretation. The Tsost Uul range is interpreted to have a half-flower structure cross-sectional geometry with the S-dipping thrust faults at the northern end of the range rooting into the steep left-lateral oblique-slip and strike-slip faults in the interior and southern end of the range (Figs. 14 and 15).

4. Gobi Bulag fault zone

This fault zone occurs adjacent to a field of volcanic vents along its central section (Fig. 2) and can be traced on the Landsat image for over 75 km. It is marked by small push-up ridges, springs and one major ridge near its western end where the system steps to the right. Four separate transects were made across the fault system at various locations to document the mechanism of uplift along the system. Efforts were also made to determine if the location and distribution of volcanic vents were in some way related to the fault system. However, no obvious alignment of vents occurs along trends that might be parallel, synthetic or antithetic splays and poor exposure between vents limits interpretation. It is possible that the vents precede fault motion.

At the eastern end of the surface expression of the fault zone, there are four low NW-trending parallel ridges covered by coarse angular boulder conglomerates and uplifted marble. They are interpreted to be small thrust ridges although the faults are not exposed (Owen et al., 1997). Fig. 18 shows two structural transects, spaced 1 km apart across a higher E–W-trending ridge that occurs 500 m to the west of the four low ridges. Both transects contain numerous E–W-striking faults that deform a low-grade metasedimentary sequence containing marble, green

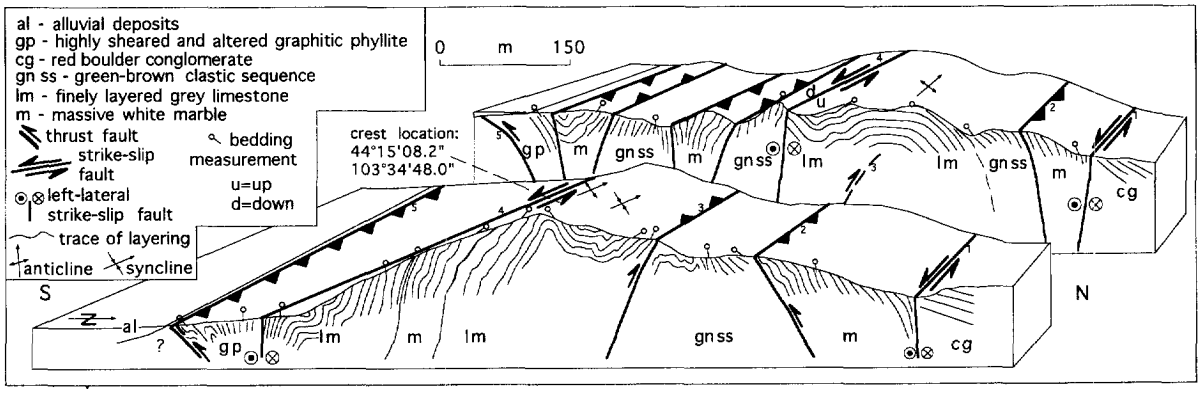

Fig. 18. Block diagrams of two structural transects made across small ridges at eastern end of the Gobi Bulag fault system. Location of figure shown in Fig. 2. Thrust, oblique-slip and strike-slip faults indicate transpressional deformation. Faults are numbered for correlation between sections.

sandstone, siliceous limestone and graphitic phyllite. The northern slope of the ridge comprises massive white Silurian marble that is in fault contact with an unmetamorphosed gently N-dipping red boulder conglomerate. The fault zone is vertical and can be traced along strike through both sections and beyond for at least several kilometres. The vertical attitude and E–W trend are consistent with it being a strike-slip fault similar to the E–W Tsost Uul fault; however, this could not be confirmed as the fault surface is not clearly exposed. The southern boundary of the ridge is marked by a highly sheared N-dipping, silver-grey graphitic phyllite. This unit is interpreted to be a thrust zone because of its highly sheared nature and because it contains numerous S-vergent minor folds. Other faults within the transects were identified by zones of truncated layering or strong brecciation. Their shear sense was determined by dragged layering, asymmetric folds adjacent to the fault or tension gash arrays. The geometry of faults and folding across both transects suggests uplift of triangular-shaped wedges in cross section bounded by thrust faults and oblique-slip strike-slip faults. Thus the ridges appear to have complex flower-geometry-shaped cross sections and some faults terminate along strike or branch and merge with other faults.

Fig. 19 shows a small transect along a stream valley that cuts through an isolated low asymmetric ridge that occurs along the length of the fault zone. At this location (44°14′46.6″N, 102°08′31.3″E), a red conglomerate with thin sandy layers is tilted approximately 30°N and is cut by numerous S-vergent brittle thrust faults. The frontal fault strikes 288, dips 52° NE and has slickensides that plunge 21°/091 suggesting left-lateral thrusting displacement.

Approximately 25 km farther west, an isolated ridge in an otherwise featureless plain occurs at a prominent right step in the fault system (Fig. 2). Fig. 20 shows a transect along a major drainage (44°14′55.2″N, 102°01′29.0″E) that cuts through the ridge and provides good exposures of the cross-sectional geology (Fig. 20). The ridge is composed of black–grey Silurian chloritic phyllites. The mountain front is marked by a steep to vertical N-dipping fault zone that emplaces the phyllite over red, fine-grained conglomerate. Bedding within the conglomerate is dragged up to vertical attitudes indicating thrusting sense motion. Slickensides are not preserved in the fault zone, thus the degree, if any, to which the fault zone has accommodated strike-slip motion is unknown. A second steep to vertical fault zone occurs approximately 180 m north of the southern mountain front and strikes 310, dips 67° NE and has slickensides that plunge 11°/125. The fault is interpreted to be a left-lateral oblique-slip fault with a thrusting component of motion. North-vergent, thrust sense kink bands (Fig. 20) are common in the frontal ridge and are interpreted to be conjugate structures to the main frontal thrust or oblique-slip thrust. Locally they are pervasive and define a crenulation cleavage.

At the northern end of the transect a steep left-lateral fault with a normal component of motion juxtaposes gently N-dipping unmetamorphosed red cobble conglomerate against the black chloritic phyllite. Along the length of the transect the trend of the foliation swings from 340–330 in the north to 300–290 at the southern mountain front. This change in trend may be due to left-lateral drag within an overall left-lateral transpressional setting.

The structural data indicate that transpressional uplift of basement phyllites has occurred along a major right-step in the Gobi Bulag fault system. Thus this isolated ridge can be regarded as a restraining

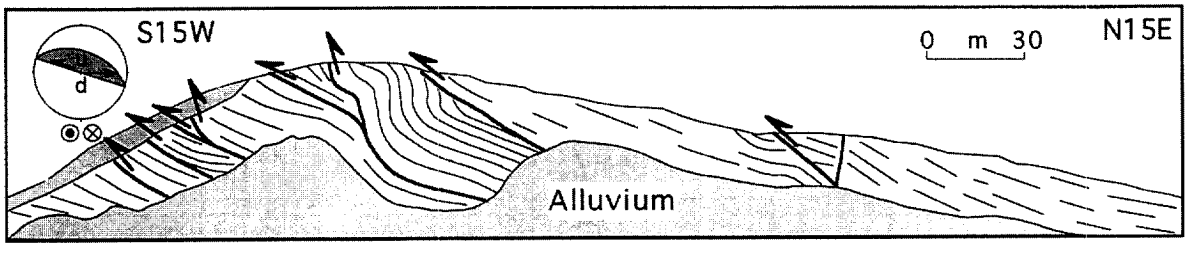

Fig. 19. Short transect across small push-up ridge of red clastic sandstones and conglomerates along the Gobi Bulag fault system. Location of figure shown in Fig. 2.

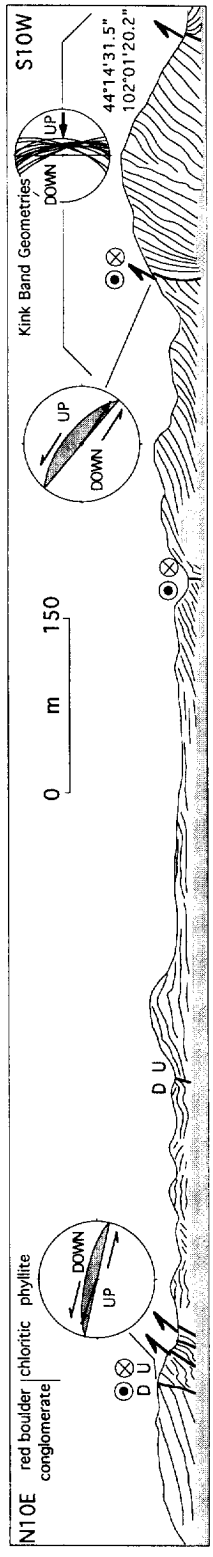

Fig. 20. Transect across small restraining bend along western segment of the Gobi Bulag fault system. Location of figure shown in Fig. 2.

bend between parallel segments of the Gobi Bulag fault system.

5. Discussion

The results of this study indicate that in the Artsa Bogd region there are distinctive domains of late Cenozoic transpressional deformation and uplift centred on major E–W fault systems (Fig. 21). The intervening corridors between Artsa Bogd and the Tsost Uul range and between the Tsost Uul range and the Gobi Bulag fault system are relatively unaffected, S-sloping subplanar, pediment surfaces. These areas are not down-dropped blocks and contain surprisingly thin (several metres to tens of metres) Cenozoic alluvial deposits. This is thought to be due to deflation by prevailing northwesterly winds that has removed considerable quantities of sediment contributing to the aeolian deposits of northern China (Traynor and Sladen, 1995).

In the Tsost Uul range and along the Gobi Bulag fault system, uplift has occurred at restraining bends along major left-lateral strike-slip faults. The uplift history of Artsa Bogd is more complex and will require more study to be fully understood. What is certain is that the range has double structural vergence, asymmetric topography and a sharply defined northern mountain front characterized by thrust and left-lateral oblique-slip faults as well as small anticlines and thrust ridges in its northern foreland that deform Quaternary sediments. The overall late Cenozoic kinematic regime is left-lateral transpres-

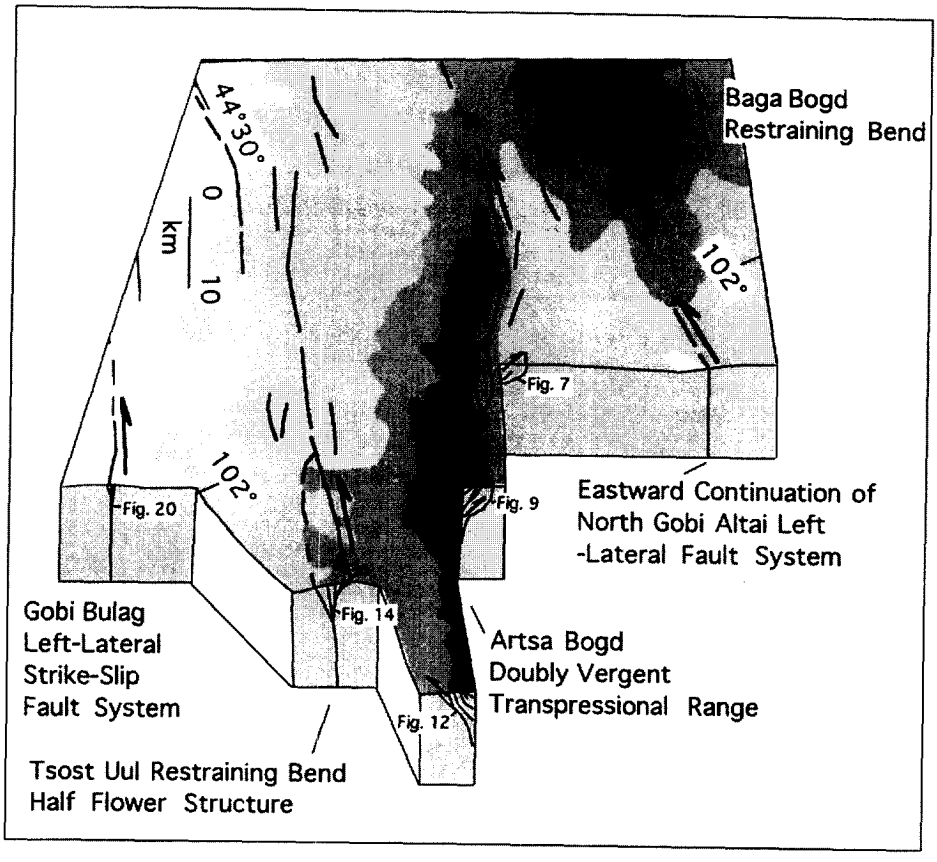

Fig. 21. Block diagram showing topography and surface fault traces observable on Landsat imagery (Fig. 2) and cross-sectional fault geometries as interpreted from this study. Major E–W-trending Artsa Bogd, Tsost Uul and Gobi Bulag fault systems define zones of localized left-lateral transpressional deformation at the eastern end of the Gobi Altai between the North Gobi Altai and Gobi Tien Shan left-lateral fault systems (Fig. 3).

sional; however, the extent to which older faults have been reactivated is unknown. The presence of thick Cretaceous clastic deposits in the region and tilted and deformed Cretaceous–Tertiary flood basalts may suggest that the Artsa Bogd region was formerly a Mesozoic depocentre, perhaps a rift basin (Samoylov et al., 1988; Traynor and Sladen, 1995) that has since been transpressionally inverted during late Cenozoic reactivation along preexisting high-angle normal faults. Further structural and stratigraphic study are needed to assess this hypothesis.

Detailed dating of past rupture events in the Artsa Bogd region is needed to ascertain whether all faults have been active concurrently or whether there has been a progressive northwards stepping of activity to the presently active North Gobi Altai fault system. The fact that the nearby North Gobi Altai fault system is seismically active and parallel to the major fault systems documented in this study raises the strong possibility that the major E–W faults in the Artsa Bogd region are still potentially active and pose a possible seismic hazard.

It is interesting to note that in the Artsa Bogd region, the major E–W strike-slip fault systems have fairly regular spacings (approximately 20 km; Fig. 21). Together the faults help define a broad corridor of Cenozoic E–W left-lateral transpressional deformation south of the Hangay Dome (Fig. 3). We speculate that the fairly regular fault spacing may be due to more diffuse E–W flow of lower crustal and lithospheric mantle material at depth and the manner in which the simple shear stresses within that flowing medium are transmitted to discrete vertical fault zones in the brittle upper crust that partition the deformation. Seismic anisotropy data for the northern Gobi Desert in this region indicate E–W fast flow directions for the lithospheric mantle (Gao et al., 1994). The ultimate driving force for the regional deformation is presumably NE-directed maximum compressive stress derived from the Indo–Eurasian collision 2500 km to the south (Tapponnier and Molnar, 1979). The easternmost Gobi Altai can be structurally linked with higher and more topographically continuous ranges in the western Gobi Altai and the easternmost Tien Shan. Thus along the Tien Shan–Gobi Altai trend, the easternmost Gobi Altai may represent the frontal zone of propagating east-northeastward transpressional deformation linked to the Indo–Eurasian collision. The fact that the mountains are low and die out to the east is probably due to diminishingly low strain rates competing with normal desert erosion rates.

References

Baljinnyam, I., Bayasgalan, A., Borisov, B.A., Cisternas, A., Dem'yanovich, M.G., Ganbataar, L., Kochetkov, V.M., Kurushin, R.A., Molnar, P., Hervé, P. and Vashchilov, Yu.Ya., 1993. Ruptures of major earthquakes and active deformation in Mongolia and its surroundings. Geol. Soc. Am. Mem., 181.

Bayarsayhan, C., Bayasgalan, A., Enhtuvshin, B., Hudnut, K.W., Kurushin, R.A., Molnar, P. and Olziybat, M., 1996. 1957 Gobi-Altay, Mongolia, earthquake as a prototype for southern California's most devastating earthquake. Geology, 24(7): 579–582.

Berkey, C.P. and Morris, K.K., 1927. Geology of Mongolia. American Museum of Natural History, New York, 475 pp.

Bull, W.B. and McFadden, L.D., 1977. Tectonic geomorphology north and south of the Garlock Fault, California. In: D.O. Doehring (Editor), Geomorphology in Arid Regions. Publications in Geomorphology, State University of New York, Binghamton, pp. 115–138.

Cunningham, W.D. and Windley, B.F., 1995. Cenozoic transpression in southwestern Mongolia and the Gobi-Altai–Tien Shan Connection. Terra Abstracts, Suppl. 1. Terra Nova, 7: 40.

Cunningham, W.D., Windley, B.F., Dorjnamjaa, D., Badamgarov, G. and Saandar, M., 1996a. Late Cenozoic transpression in southwestern Mongolia and the Gobi Altai–Tien Shan connection. Earth Planet. Sci. Lett., 140: 67–82.

Cunningham, W.D., Windley, B.F., Dorjnamjaa, D., Badamgarov, G. and Saandar, M.A., 1996b. Structural transect across the Mongolian Altai: active transpressional mountain building in central Asia. Tectonics, 15(1): 142–156.

Dergunov, A.B., 1989. Caledonides in central Asia. Nauka, Moscow, 191 pp. (in Russian).

Devyatkin, E.V., 1974. Structures and formational complexes of the Cenozoic activated stage (in Russian). In: Tectonics of the Mongolian People's Republic. Nauka, Moscow, pp. 182–195.

Devyatkin, E.V., 1975. Neotectonic structures of western Mongolia (in Russian). In: Mesozoic and Cenozoic Tectonics and Magmatism of Mongolia. Nauka, Moscow, pp. 264–282.

Florensov, N.A. and Solonenko, V.P. (Editors), 1963. The Gobi Altai Earthquake (in Russian). Akademie Nauk, Moscow (English translation. U.S. Department of Commerce, Washington, D.C., 424 pp. (1965).

Gao, S., Davis, P.M., Liu, H., Slack, P.D., Zorin, Yu.A., Mordvinova, V.V., Kozhavnikov, V.M. and Meyer, R.P., 1994. Seismic anisotropy and mantle flow beneath the Baikal rift zone. Nature, 371: 149–151.

Hendrix, M.S., Graham, S.A., Amory, J.Y. and Badarch, G., 1996. Noyon Uul syncline, southern Mongolia: Early Mesozoic sedimentary record of the tectonic amalgamation of central Asia. Bull. Geol. Soc. Am., 108: 1256–1274.

Khilkho, S.D., Kurushin, R.A., Kochetkov, V.M., Balzhinnyam,

I. and Monkoo, D., 1985. Strong earthquakes, paleoseismogeological and macroseismic data. In: Earthquakes and the Bases for Seismic Zoning of Mongolia. Transactions 41, the Joint Soviet–Mongolian Scientific Geological Research Expedition, Nauka, Moscow, pp. 19–83.

Lamb, M.A. and Badarch, G., 1995. The arc mess monster: sedimentation, volcanism and tectonics of southern Mongolia during the Palaeozoic. Geol. Soc. Am., Abstr. Progr., A-391.

Owen, L.A., Windley, B.F., Cunningham, W.D., Badamgarov, J. and Dorjnamjaa, D., 1997. Quaternary alluvial fans in the Gobi Desert, southern Mongolia: Evidence for neotectonics and climate change. J. Quat. Sci., in press.

Ruzhentsev, S.V. and Badarch, G., 1989. Preorogenic tectonics of southern Mongolia. Dokl. Akad. Nauk SSSR, 305(3): 682–685.

Samoylov, V.S., Ivanov, V.G., Arakelyants, M.M., Frikh-khap, D.I. and Yarmolyuk, V.V., 1988. Late Mesozoic magmatism of the Artsa Bogd region (Gobi Altai, Mongolia). Geological Series, 11, pp. 14–26.

Sengör, A.M.C., Natal'in, B.A. and Burtman, V.S., 1993. Evolution of the Altaid tectonic collage and Palaeozoic crustal growth in Eurasia. Nature, 364: 299–307.

Shuvalov, V.F., 1969. Continental red beds of the Upper Jurassic of Mongolia. Dokl. Akad. Nauk, SSSR, 189(5): 1088–1091.

Suyetenko, O.D., Golovchenko, Ye.V. and Eenzhin, G., 1978. Paleozoic tectonic nappes on the eastern spurs of the Gobi Altai (Southern Mongolia). Geotectonics, 12(5): 384–391.

Tapponnier, P. and Molnar, P., 1979. Active faulting and Cenozoic tectonics of the Tien Shan, Mongolia, and Baykal regions. J. Geophys. Res., 84: 3425–3459.

Tikhonov, V.I. and Yarmolyuk, V.V., 1982. Structure and evolution of the Gobi Altai, southern boundary structure of the Mongolian Caledonides. Geotectonics, 16(4): 266–273.

Traynor, J.J. and Sladen, C., 1995. Tectonic and stratigraphic evolution of the Mongolian People's Republic and its influence on hydrocarbon geology and potential. Mar. Pet. Geol., 12: 35–52.

Yarmolyuk, V.V., Kovalenko, V.I. and Samoylov, V.S., 1991. Tectonic setting of the late Cenozoic volcanism in central Asia. Geotectonics, Jan.-Feb. No.1: 69–83.

Zorin, Y.A., Belichenko, V.G., Turutanov, E.Kh., Kozhevnikov, V.M., Ruzhentsev, S.V., Dergunov, A.B., Filippova, I.B., Tomurtogoo, O., Arvisbaatar, N., Bayasgalan, Ts., Biambaa, Ch. and Khosbayar, P., 1993. The south Siberia–central Mongolia transect. Tectonophysics, 225: 361–378.